Design, fabrication and characterization of MoS_2 self-lubricating pure MoS_2 Coatings for space applications using PVD magnetron sputtering

M. F. Wani[1*], *Umida* Ziyamukhamedova[2], *Taseer A.* Mufti[1], *Rakesh* Sehgal[1], and *Sheikh S.* Saleem[1]

[1]National Institute of Technology Srinagar, Kashmir, India
[2]Tashkent State Transport University, Tashkent, Uzbekistan

Abstract. Tribological components cost just a fraction of the whole spacecraft, but they often lead to failures that partially or completely disrupt the spacecraft. Mechanical components used in space applications have to withstand extreme and severe environmental conditions such as very high or very low cryogenic temperatures, high vacuum, corrosive elements and radiation. MoS_2 is the most widely used lubricating material in space applications. It possesses a lamellar structure with strong covalent bonds within layers and simultaneously weak van der Wall's interlayer bonds, resulting in easy shearing of the crystals in the direction parallel to the basal planes, hence acting as a good solid lubricant.
In this research, a thin film nano scale coating of MoS_2 was deposited on steel using Physical Vapour Deposition (PVD). The PVD technique used was the RF magnetron sputtering process. Material characterization was performed using X-Ray diffraction (XRD), Field Emission Scanning Electron Microscopy (FESEM) and Raman spectroscopy.
According to the results, the developed MoS_2 nano coatings have a polycrystalline structure with basal planes that are oriented perpendicular to the substrate surface.

1 Introduction

Solid-based lubricating thin films consist of single or multilayer solid or composite materials that are used to reduce friction and wear between interacting surfaces. To provide lubrication and minimize friction and wear, solid lubricants should have certain basic properties, i.e. low shear strength, good adherence to the substrate material, they should be softer than the material to which they should be applied (low abrasivity) and they should be thermodynamically stable throughout the operating temperature range [1-4].

MX_2 represents the class of materials known as transition metal dichalcogenides (where M represents D block elements of the periodic table also known as transition metals and X represents the elements in group 16 of the periodic table known as chalcogens). MX_2 has a hexagonal crystal structure with each M layer sandwiched between two X layers in each monolayer. 2H (hexagonal) and 1T (trigonal) are the most common coordinations in

* Corresponding author: mfwani@nitsri.ac.in

TMDCs around M atoms [5-7]. Similar to graphite and hBN, the bulk MX_2 layers are joined by weak van der Walls forces. This results in weak shear strength in a direction parallel to the basal planes [8-10].

Bulk MoS_2 exists in a large number of distinct crystal structures (polymorphs) depending on the relative arrangement of the S and Mo atoms in the layer and on the subsequent layers. The most common polymorphs identified so far are 2H (hexagonal)-MoS_2 and 3R (rhombohedral)-MoS_2 both of which have trigonal prismatic coordination around Mo atoms. The polymorphic parameters and properties are shown in Table 1.

AMS 5898 is a highly corrosion resistant, pressure-nitrided martensitic stainless steel. Some of the features the material has to offer are hardness up to 60 HRC combined with outstanding toughness. Compared to normal stainless steels, it has outstanding resistance to corrosion and wear. It provides a high tempering resistance of up to 500°C [11-18].

Table 1. Parameters and properties of MoS_2polymorphs [19]

Polymorph	Space Group	Point Group	Atoms Per Cell	Stacking	Lattice Parameters	Properties
1T	$P\bar{3}m1$	D_{3d}	9	AAAAAA	a =5.60 Å c =5.99 Å	metallic, metastable
2H	$P6_3/mmc$	D_{6h}	6	ABABAB	a =3.16 Å c =12.29 Å	semiconducting, naturally occurring
3R	R3m	C_{3v}	9	ABCABC	a =3.17 Å c =18.38 Å	semiconducting, naturally occurring

AMS 5898 is a comparatively recent material used to make anti friction bearings. Anti-friction bearings made of this material exhibit improved fatigue life and better corrosion resistance compared to standard anti friction bearing materials used in space applications.

2 Materials and methods

Based on the comprehensive literature review it is clear that detailed nanomechanical and tribological studies of MoS_2 nanocoating on AMS 5898 steel substrates have yet to be performed. As a result, the material and coatings chosen for this study are AMS 5898 and MoS_2, respectively.

The raw material AMS 5898 was purchased from *Tech Steel & Materials (Holbrook, New York, USA)*. The material was in the form of a rod having diameter of 27 mm and length of 254 mm. The weight of the rod was measured to be 1.14 Kg.

The chemical composition and mechanical properties of AMS 5898 has been provided in Table 2 and Table 3 respectively.

Table 2. Chemical Composition of AMS 5898

Element	Mo	Si	Mn	N	C	Cr	Va	Cu	Al	Fe
Weight %	0.98-0.99	0.64-0.66	0.36-0.37	0.38-0.39	0.30	15.42-15.50	0.04	0.07	0.005-0.006	Balance

Table 3. Mechanical Properties of AMS 5898

№	Property	Value
1	Tensile Strength	2150 MPa
2	Yield Strength	1850 MPa
3	Hardness	59 HRC
4	Elongation	3%
5	Toughness	>20 [MPa $\sqrt{m}$]

The samples from rod of 25mm diameter were cut to a thickness of 10mm and were polished with a Bainpol Auto automatic polishing machine to a mirror-like finish. The samples were polished first with various emery papers and then with diamond pastes. Emery papers with grit sizes of 320, 400, 600, 800, and 1000 were used for polishing, followed by polishing with 3, 1, 0.25 µm diamond pastes.

The samples were then ultrasonically cleaned in an acetone bath for 5 minutes and dried in an oven for 5 minutes at 50°C. After cleaning the surface of the samples was observed under an optical microscope and surface roughness was measured using a 3D profilometer.

The coating was deposited using a PVD magnetron sputtering process. The sputtering process was carried out using MiniLab 060 by Moorfield Nanotechnology UK at CRFC Lab NIT Srinagar.

In order to remove any contamination and to improve coating adhesion the substrate was pre-etched by Argon for 10 minutes at 45 Watt RF power before coating deposition. The process chamber was evacuated to base pressure of 5×10^{-7} mbarby a turbo-molecular pump while only Argon was allowed to enter the chamber during the deposition process. The details of coating deposition are listed in Table 4.

Table 4. Details of coating deposition

Substrate heating	No
Deposition temperature	18°C
Working Pressure	4×10^{-3} mbar
Power	50 W (RF)
Ar flow	4.2 sccm
Deposition time	20 minutes
Target to substrate distance	16 cm (approx)
Coating thickness	*76 m*

Characterization of deposited coatings involves determining the film thickness, chemical composition, crystallographic structure, and surface morphology.

The topographical and 3D surface images, surface roughness and coating thickness were determined using an Rtec 3D optical profilometer with AFM and optical microscope (Leica DM6000 M). Furthermore, the surface roughness, R_a, of the polished samples and coatings was calculated using Gwyddion and Hystriontriboview software.

X-ray diffraction (XRD) technique is the most commonly used for determining the crystallographic structure of coatings. It provides details on the crystal orientation, phases present, lattice parameters, crystal structure, degree of crystallinity, etc.

The XRD pattern of the base material and the coatings were recorded using a Rigaku SmartLab X-ray diffractometer. The X-ray diffractogram pattern was compared with the ICDD powder diffraction database using Rigaku's PDXL integrated XRD software.

However, the X-ray diffraction pattern of the coating was determined using GIXRD to avoid any interference from the substrate.The gazing incidence angle was fixed to 0.8° and the diffraction was measured from 5° to 80°, with a step width of 0.04°. The X-ray diffractogram pattern of the coating was also compared with the ICDD database.

FESEM has the benefit of being able to produce high resolution images. This improves the ability to observe ultrafine surface properties. FESEM images of the substrate material (AMS 5898) and the

coating was obtained using ZEISS GeminiSEM 500. During the whole process the system vacuum was maintained below 1×10^{-5} mbar.

The chemistry and crystal structure of MoS_2 coatings were determined using Raman spectroscopy. The Raman analysis in this study was performed at the CRFC Lab, NIT Srinagar, using a Renishaw inVia Raman microscope. A focused green laser beam with a wavelength of 532 nm was used to acquire Raman spectra of the coating. The laser power was set to 50 mW with a 60 second exposure time, and the spectrum was acquired from 0 to 3200 cm-1.

3 Results and discussion

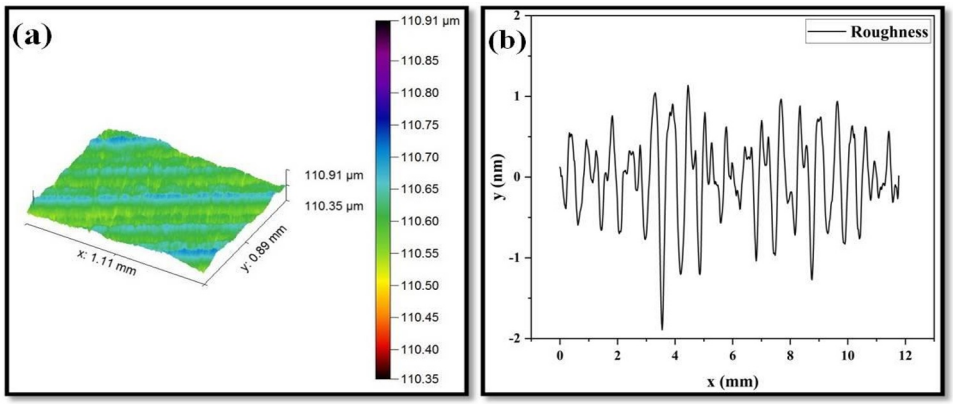

Fig. 1. (a) 3D surface topographical image and (b) Surface roughness of a representative sample

The substrate material (AMS 5898) after machining to the required dimensions was polished to a mirror like finish. The surface roughness of all the samples was less than 10 nm. The 3D surface topographical image and the surface roughness of a representative sample are shown in Figure 1 (a) and (b) respectively. The figure shows that the surface is evenly polished and has a smooth texture, and the average surface roughness, Ra, of this sample is measured to be 5.618 nm.

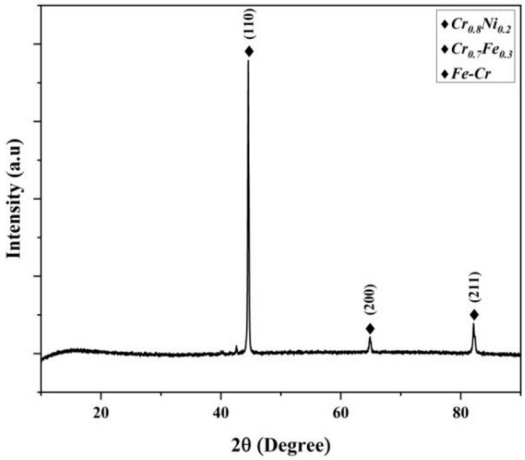

Fig. 2. X-Ray diffractogram of AMS 5898

A Cu-Kα radiation (λ= 1.5406Å) at 40 kV and 30 mA was used to generate the X-Ray diffractogram of the material and the diffraction pattern was recorded for 2θ ranging from 10° to 90°. Figure 2 represents the X-ray diffractogram of AMS 5898. The crystal structure of AMS 5898 is highly crystalline, with prominent peaks at 2θ values corresponding to 44.55°, 64.85°, and 82.14°.

The FESEM micrographs of nanocoating show that a uniform coating of MoS_2 has been successfully developed and exhibits a consistent floral or worm-like morphology [20-28]. The coating features a lamellar structure with MoS_2 basal planes (002) developed perpendicular to the substrate but randomly oriented. Fig. 3 depicts the FESEM images of MoS_2 nanocoating at different magnifications.

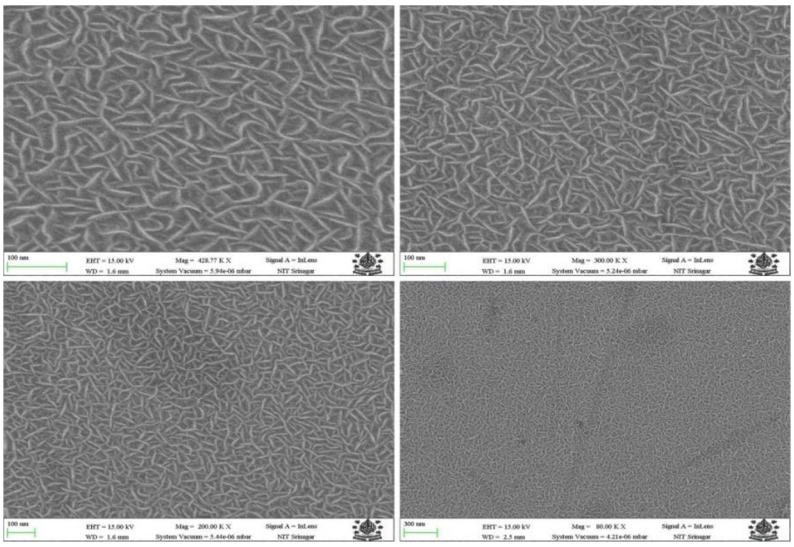

Fig. 3. FESEM Images of MoS_2 nanocoating at different magnifications

The GIXRD of the nanocoating is shown in Fig. 4 (a). It depicts that the deposited MoS_2 nanocoating has a polycrystalline structure with crystal growth along several directions. It has typical diffraction peaks of (002), (100) and (110) at 2θ values of 13.87°, 33.3° and 58.63° corresponding to 2H- MoS_2[29-34].

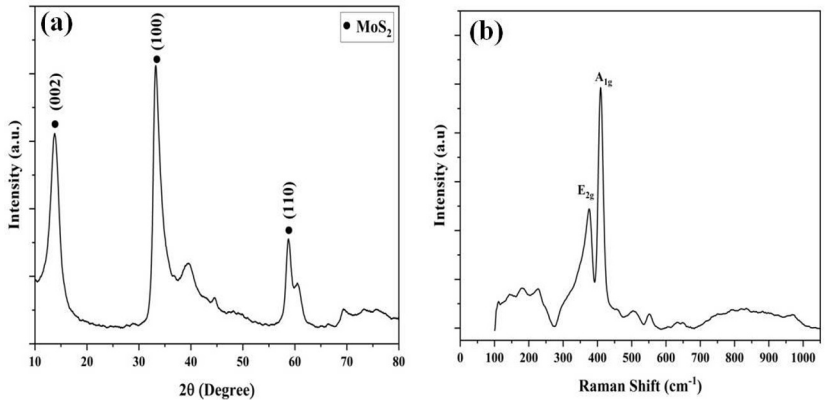

Fig. 4. (a) GIXRD and (b) Raman spectrum of MoS_2 nanocoating

The Raman spectrum of the MoS_2 nanocoating is displayed in Figure 4 (b). The spectra reveal two notable peaks of E2g mode at 375 cm-1 and A1g mode at 409 cm-1. The E2g mode is formed by the vibration of S and Mo atoms in different directions but in the same plane, whereas the A1g mode is formed by the out of plane vibration of S atoms only. Depending on the number of MoS_2 layers these peaks may shift slightly towards left or right [35-40]. Therefore, Raman peaks corresponding to E2g and A1g modes confirm the presence of MoS_2.

The surface roughness of the coating was evaluated using Scanning Probe Microscope (SPM) imaging and the average surface roughness (Ra) was measured to be 4.21 nm as shown in Fig. 5.

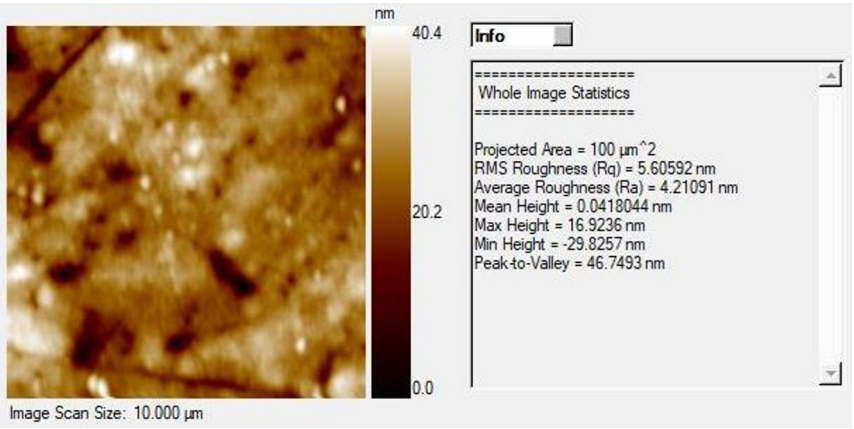

Fig. 5. Surface roughness of MoS_2 nanocoating

4 Conclusions

In this study, the material characteristics of the MoS_2 coating were evaluated. The coating was deposited on AMS 5898 steel substrate using a magnetron sputtering process. The coating was characterized using XRD, FESEM and Raman spectroscopy. The developed coating has a polycrystalline structure with pronounced peaks (002), (100), and (110) corresponding to MoS2. The FESEM image showed that the developed MoS2 coating has a worm or flower structure with basal planes developed perpendicular to the substrate. The Raman spectrum of the coatings shows two notable peaks of E_{2g} mode at 375 cm^{-1} and A_{1g} mode at 409 cm^{-1}, thus confirming the presence of MoS_2.

References

1. Campbell M E 1998 Campbell, M. E. (1998). Technology Utilization - SOLID LUBRICANTS. NASA Technical Memorandum, (01). NASA Technical Memorandum 5059
2. Kasneci G, Elbassuoni S and Weikum G 2009 Solid Lubricants and Coatings for Extreme Environments: State-of-the-Art Survey Proceeding of the 18th ACM conference on Information and knowledge management - CIKM '09 (New York, New York, USA: ACM Press) p 1653. DOI: 10.1145/1645953.1646196
3. Gresham R M 2018 ASM HANDBOOK Volume 18: Friction, Lubrication, and Wear

Technology Tribology & Lubrication Technology74 84

4. Novoselov K S, Mishchenko A, Carvalho A and Castro Neto A H 2016 2D materials and van der Waals heterostructures Science353 aac9439. DOI: 10.1126/science.aac9439
5. Somvanshi D and Jit S 2020 5 - Transition metal dichalcogenides based two-dimensional heterostructures for optoelectronic applications Micro and Nano Technologies ed S Jit and S B T-2D N H M Das (Elsevier) pp 125–49. DOI: https://doi.org/10.1016/B978-0-12-817678-8.00005-1
6. Hilton M R and Fleischauer P D 1992 Applications of solid lubricant films in spacecraft Surface and Coatings Technology 54–55 435–41. DOI: https://doi.org/10.1016/S0257-8972(07)80062-4
7. Bowden F P and Tabor D 1951 The Friction and Lubrication of Solids American Journal of Physics 19 428–9. DOI: 10.1119/1.1933017
8. Spalvins T 1987 A review of recent advances in solid film lubrication Journal of Vacuum Science & Technology A: Vacuum, Surfaces, and Films 5 212–9. DOI: 10.1116/1.574106
9. Bowden F P, Bowden F P and Tabor D 2001 The friction and lubrication of solids vol 1 (Oxford university press)
10. Magnéli A 1953 Structures of the ReO3-type with recurrent dislocations of atoms: `homologous series' of molybdenum and tungsten oxides Acta Crystallographica 6 495–500. DOI: https://doi.org/10.1107/S0365110X53001381
11. Vaziriserehk M R, Martini A, Strubbe D A and Baykara M Z 2019 Solid lubrication with MoS_2: A review Lubricants7 57
12. Righton Blackburns Limited Data Sheet: Cronidur 30 - AMS 5898 - 1.4108 | Righton Blackburns Limited. Rightonblackburns.co.uk. Published 2019. Accessed Nov 13, 2020. https://www.rightonblackburns.co.uk/datasheets/view/Righton-Blackburns-Ltd_Bearing-Steels-Cronidur-30-AMS-5898-14108_
13. Anon 2001 Cronidur 30. (2001). Aircraft Engineering and Aerospace Technology, 73(1), 230–239. Aircraft Engineering and Aerospace Technology 73 aeat.2001.12773aad.014. DOI: 10.1108/aeat.2001.12773aad.014
14. FAG OEM und Handel AG Index of /PDF_catalogues/FAG. Ahrinternational.com. Published 2012. Accessed Feb 16, 2021. https://www.ahrinternational.com/PDF_catalogues/FAG/FAG_rolling_bearings_made_from_cronidur_30.pdf (Georg-Schäfer-Str. 30)
15. Brainard W A 1968 The thermal stability and friction of the disulfides, diselenides, and ditellurides of molybdenum and tungsten in vaccum (10-9 to 10-6 TORR) NASA Technical Note D-5141 1–26
16. Jamison W E and Cosgrove S L 1971 Friction Characteristics of Transition-Metal Disulfides and Diselenides A S L E Transactions 14 62–72. DOI: 10.1080/05698197108983228
17. Joly-Pottuz L and Iwaki M 2007 Superlubricity of Tungsten Disulfide Coatings in Ultra High Vacuum Superlubricity ed A Erdemir and J-M B T-S Martin (Amsterdam: Elsevier) pp 227–36. DOI: 10.1016/B978-044452772-1/50045-7
18. Briscoe B J and Evans D C B 1982 SHEAR PROPERTIES OF LANGMUIR-BLODGETT LAYERS. Proceedings of The Royal Society of London, Series A: Mathematical and Physical Sciences 380 389–407. DOI: 10.1098/rspa.1982.0048
19. Stupp B C 1981 Synergistic effects of metals co-sputtered with MoS_2Thin Solid

Films84 257–66. DOI: 10.1016/0040-6090(81)90023-7

20. Fleischauer P D 1984 Effects of crystallite orientation on environmental stability and lubrication properties of sputtered moSASLE Transactions27 82–8. DOI: 10.1080/05698198408981548
21. Donnet C, Le Mogne T and Martin J M 1993 Superlow friction of oxygen-free MoS_2 coatings in ultrahigh vacuum Surface and Coatings Technology 62 406–11. DOI: https://doi.org/10.1016/0257-8972(93)90275-S
22. Oviedo J P, KC S, Lu N, Wang J, Cho K, Wallace R M and Kim M J 2015 In Situ TEM Characterization of Shear-Stress-Induced Interlayer Sliding in the Cross Section View of Molybdenum Disulfide ACS Nano 9 1543–51. DOI: 10.1021/nn506052d
23. Hao R, Tedstone A A, Lewis D J, Warrens C P, West K R, Howard P, Gaemers S, Dillon S J and O'Brien P 2017 Property Self-Optimization During Wear of MoS 2 ACS Applied Materials & Interfaces 9 1953–8. DOI: 10.1021/acsami.6b13802
24. Onodera T, Morita Y, Nagumo R, Miura R, Suzuki A, Tsuboi H, Hatakeyama N, Endou A, Takaba H, Dassenoy F, Minfray C, Joly-Pottuz L, Kubo M, Martin J-M and Miyamoto A 2010 A Computational Chemistry Study on Friction of h-MoS2. Part II. Friction Anisotropy The Journal of Physical Chemistry B 114 15832–8. DOI: 10.1021/jp1064775
25. Peterson M B and Johnson R L 1953 Friction and Wear Investigation of Molybdenum Disulfide: I--Effect of Moisture National Advisory Committee for Aeronautics
26. Panitz J K G, Pope L E, Lyons J E and Staley D J 1988 The tribological properties of MoS_2 coatings in vacuum, low relative humidity, and high relative humidity environments Journal of Vacuum Science & Technology A 6 1166–70. DOI: 10.1116/1.575669
27. Baker R T K, Chludzinski J J and Sherwood R D 1987 In-situ electron microscopy study of the reactivity of molybdenum disulphide in various gaseous environments Journal of Materials Science 22 3831–42. DOI: 10.1007/BF01133329
28. Khare H S and Burris D L 2013 The Effects of Environmental Water and Oxygen on the Temperature-Dependent Friction of Sputtered Molybdenum Disulfide Tribology Letters 52 485–93. DOI: 10.1007/s11249-013-0233-8
29. Gao X, Hu M, Sun J, Fu Y, Yang J, Liu W and Weng L 2015 Changes in the composition, structure and friction property of sputtered MoS_2 films by LEO environment exposure Applied Surface Science 330 30–8. DOI: 10.1016/j.apsusc.2014.12.175
30. Bichsel R, Buffat P and Levy F 1986 Correlation between process conditions, chemical composition and morphology of MoS_2 films prepared by RF planar magnetron sputtering Journal of Physics D: Applied Physics19 1575–85. DOI: 10.1088/0022-3727/19/8/025
31. Li H, Xie M, Zhang G, Fan X, Li X, Zhu M and Wang L 2018 Structure and tribological behavior of Pb-Ti/MoS2 nanoscaled multilayer films deposited by magnetron sputtering method Applied Surface Science 435 48–54. DOI: 10.1016/j.apsusc.2017.10.170
32. Wei C-Y, Lee P-C, Tsao C-W, Lee L-H, Wang D-Y and Wen C-Y 2020 In situ Scanning Electron Microscopy Observation of MoS2 Nanosheets during Lithiation in Lithium Ion Batteries ACS Applied Energy Materials 3 7066–72. DOI: 10.1021/acsaem.0c01102
33. Pope L E and Panitz J K G 1988 The effects of hertzian stress and test atmosphere on the friction coefficients of MoS_2 coatings Surface and Coatings Technology 36 341–

50. DOI: 10.1016/0257-8972(88)90164-8

34. Lovell M R, Khonsari M M and Marangoni R D 1997 Frictional Analysis of MoS_2 Coated Ball Bearings: A Three-Dimensional Finite Element Analysis Journal of Tribology 119 754–63. DOI: 10.1115/1.2833881
35. Scharf T W, Kotula P and Prasad S V 2010 Friction and wear mechanisms in MoS_2/Sb_2O_3/Au nanocomposite coatings Acta Materialia 58 4100–9. DOI: 10.1016/j.actamat.2010.03.040
36. Asmoro G, Surojo E, Ariawan D, Muhayat N and Raharjo W W 2018 Role of solid lubricant (MoS_2 and graphite) variations on characteristics of b3ake lining composite IOP Conference Series: Materials Science and Engineering 420 012022. DOI: 10.1088/1757-899X/420/1/012022
37. Singer I L, Bolster R N, Wegand J, Fayeulle S and Stupp B C 1990 Hertzian stress contribution to low friction behavior of thin MoS_2 coatings Applied Physics Letters 57 995–7. DOI: 10.1063/1.104276
38. Li H, Xie M, Zhang G, Fan X, Li X, Zhu M and Wang L 2018 Structure and tribological behavior of Pb-Ti/ MoS_2nanoscaled multilayer films deposited by magnetron sputtering method Applied Surface Science435 48–54. DOI: 10.1016/j.apsusc.2017.10.170
39. Curry J F, Wilson M A, Luftman H S, Strandwitz N C, Argibay N, Chandross M, Sidebottom M A and Krick B A 2017 Impact of Microstructure on MoS2 Oxidation and Friction ACS Applied Materials & Interfaces 9 28019–26. DOI: 10.1021/acsami.7b06917
40. Wei C-Y, Lee P-C, Tsao C-W, Lee L-H, Wang D-Y and Wen C-Y 2020 In situ Scanning Electron Microscopy Observation of MoS_2 Nanosheets during Lithiation in Lithium Ion Batteries ACS Applied Energy Materials3 7066–72. DOI: 10.1021/acsaem.0c01102